THE JOURNAL OF COMPARATIVE NEUROLOGY 420:512–526 (2000)

# Localization of Choline Acetyltransferase in the Developing and Adult Turtle Retinas

LYNETTE T. NGUYEN,[1] JOAQUIN DE JUAN,[2] MARIA MEJIA,[1] AND NORBERTO M. GRZYWACZ[1]*
[1]The Smith-Kettlewell Eye Research Institute, San Francisco, California 94115
[2]Departamento de Biotecnología, Facultad de Ciencias, Universidad de Alicante, 03080 Alicante, Spain

ABSTRACT

Acetylcholine has important epigenetic roles in the developing retina. In this study, cells that expressed choline acetyltransferase (ChAT), the enzyme that synthesizes acetylcholine, were investigated in embryonic, postnatal, and adult turtle retinas by using immunofluorescence histochemistry. ChAT was present at stage 15 (S15) in cells near the vitreal surface. With the formation of the inner plexiform layer (IPL) at S18, ChAT-immunoreactive (-IR) cells were located in the inner nuclear layer (INL) and the ganglion cell layer (GCL). In the INL, presumed starburst amacrine cells were homogenous in appearance and formed a single row next to the IPL: This pattern was conserved until adulthood. In the GCL, however, there were multiple rows of ChAT-IR cells early in development, and this high density of labeled cells continued during the embryonic stages, until around birth. The high density of ChAT-IR cells in the GCL was due in part to a population of cells that expressed ChAT transiently. In postnatal stages and adult retinas, the presumed starburst amacrine ChAT-IR cells formed two mirror-like rows of homogenous cells on both borders of the IPL. Two cholinergic dendritic strata that were continuous with these cells were observed as early as S18, and their depths in the IPL were relatively stable throughout development. A third population of ChAT-IR cells was observed toward the middle of the INL around S25 and persisted into adulthood. Finally, cells in the outer nuclear layer (ONL) were ChAT-IR during the embryonic stages, were less immunoreactive during the postnatal stages, and were not immunoreactive in the adult retinas. J. Comp. Neurol. 420:512–526, 2000. © 2000 Wiley-Liss, Inc.

**Indexing terms: amacrine cells; choline acetyltransferase; cell density; development; fluorescence microscopy; immunohistochemistry, photoreceptor cells; retinal ganglion cells; starburst amacrine cells; transient population; turtles; vertebrates**

A small population of amacrine cells in the adult vertebrate retina synthesizes acetylcholine (Masland and Livingstone, 1976; Masland and Mills, 1979) and releases acetylcholine (Masland and Livingstone, 1976; Masland and Mills, 1979; Massey and Redburn, 1982). To date, cholinergic amacrine cells have been identified in neonatal and adult vertebrates, including human (Hutchins and Hollyfield, 1987), monkey (Mariani and Hersh, 1988), cat (Schmidt et al., 1985; Pourcho and Osman, 1986; Dann, 1989), rat (Voigt, 1986), pig (Eckenstein and Thoenen, 1982), rabbit (Masland and Mills, 1979; Masland et al., 1984), tree shrew (Conley et al., 1986; Sandman et al., 1997), chicken (Millar et al., 1985, 1987), dogfish (Brandon, 1991), goldfish (Famiglietti and Tumosa, 1987), and turtle (Criswell and Brandon, 1992; Guiloff and Kolb, 1992). These cells make direct connections to ganglion cells (Famiglietti, 1983b) and, thus, directly shape how visual stimuli are processed. In the adult retina, these cholinergic cells are synonymous with the well-described starburst amacrine cells (Famiglietti, 1983a; Vaney, 1984; Tauchi and Masland, 1984), which have a role in directional selectivity (Ariel and Daw, 1982; Vaney, 1990;

Grant sponsor: National Eye Institute: Grant numbers: EY08921 and EY11170; Grant sponsor: DGICYT; Grant number: PB-96-0414.

*Correspondence to: Dr. Norberto M. Grzywacz, The Smith-Kettlewell Eye Research Institute, 2318 Fillmore Street, San Francisco, CA 94115. E-mail: nmg@ski.org

Received 30 March 1999; Revised 13 January 2000; Accepted 13 January 2000

© 2000 WILEY-LISS, INC.

Famiglietti, 1992; Grzywacz et al., 1998). Starburst amacrine cell bodies are located near both borders of the inner plexiform layer (IPL). Dendritic processes from those cells that are located in the proximal region of the inner nuclear layer (INL) ramify in sublamina a of the IPL (Famiglietti, 1983b; Famiglietti and Tumosa, 1987) at the border of strata 1 (s1) and s2 (Guiloff and Kolb, 1992) and make synaptic connections with OFF and ON/OFF-center ganglion cells (Famiglietti, 1987). By contrast, cells that are located in the ganglion cell layer (GCL) send their processes to sublamina b of the IPL (Famiglietti, 1983b; Famiglietti and Tumosa, 1987) at the s3–s4 border (Guiloff and Kolb, 1992) and make synaptic connections with ON and ON/OFF-center ganglion cells (Famiglietti, 1987).

In the developing retina, acetylcholine has been suggested to have epigenetic roles. Acetylcholine plays a role in spontaneous activity in the turtle (Sernagor and Grzywacz, 1999), rabbit (Masland, 1977; Zhou, 1998), chicken (Catsicas et al., 1998), and ferret (Feller et al., 1996) retinas. Hence, acetylcholine may be an environmental factor that helps to translate genetic information into retinal ontogeny. Spontaneous bursts of activity occur in immature ganglion cells. These bursts result in waves of correlated activity across the retinas (Galli and Maffei, 1988; Meister et al., 1991; Sernagor and Grzywacz, 1995; Wong et al., 1993, 1995). It is during this period that the ganglion cells generate early synaptic connections to the extraretinal areas of the brain (Penn et al., 1998). Therefore, spontaneous bursts may play a role in the refinement of these synaptic connections (Penn et al., 1998). Recent findings have demonstrated that acetylcholine, acting through nicotinic receptors at the ganglion cell membrane, is necessary for generating these spontaneous bursts (Copenhagen, 1996; Feller et al., 1996; Sernagor and Grzywacz, 1996; Sernagor and Grzywacz, 1999). Furthermore, acetylcholine may play an important role in the expansion of receptive field size of ganglion cells during the late embryonic and early neonatal stages (Sernagor and Grzywacz, 1996). Other possible roles of acetylcholine in the developing retina include growth and differentiation (Wong, 1995), cell-to-cell communication (Bussolino et al., 1988), and synaptogenesis (Ma and Grant, 1984). At later stages of development, acetylcholine may play a role in the maintenance of synaptic structures (Lipton and Kater, 1989).

Understanding the development of the retina cholinergic system will help to elucidate some of its epigenetic roles and may constrain hypothesis for its role in the adult visual processing. In the current study, immunofluorescence labeling of choline acetyltransferase (ChAT) was identified in the turtle retina from stage 14 [S14; approximately embryonic day 15 (E15) in a 60-day embryonic period] to adulthood. Localization of ChAT in developing turtle retinas includes but is not restricted to the presumed starburst cholinergic amacrine cells.

## MATERIALS AND METHODS

Data in this study were obtained from turtle (*Trachemys Scripta elegans*) retinas at varying developmental stages (S14 to adult) supplied by Kliebert (Hammond, LA). The turtles' developmental stages were determined by using criteria outlined by Yntema (1968). All procedures were performed in compliance with the National Institutes of Health Guide for the Care and Use of Laboratory Animals. Turtle eggs were kept in a humid incubator maintained at 29°C and were rotated daily until their appropriate developmental stage. Postnatal and adult turtles were kept on a 12-hour light-dark cycle and received food and water ad libitum. Following the surgical techniques of Sernagor and Grzywacz (1995), animals were decapitated and pithed, and the eyes were removed quickly and bisected. The posterior chambers were isolated and immersed in cold 4.0% paraformaldehyde (Sigma, St. Louis, MO) in 0.1 M phosphate buffer (PB), pH 7.4, for 4 hours to overnight at 4°C. Eye cups were washed through several changes of PB, pH 7.4, and cryoprotected in 15% sucrose (Sigma) overnight at 4°C. The following day, the eye cups were embedded in cryomolds and frozen in isopentane (Sigma) cooled in a chamber of liquid nitrogen. Vertical sections of the retina were cut with a cryostat at 10–14 μm, collected on microscopic slides that were pretreated with chrom-alum gelatin, and processed for immunofluorescence histochemistry. For the localization of ChAT, sections first were blocked with 4.0% normal horse serum (NHS) in PB, pH 7.4, for 1 hour at room temperature followed by incubation with affinity-purified goat anti-ChAT (Chemicon, Temecula, CA) in 1.0% NHS/PB, pH 7.4, at a dilution of 1:800–1:1600 in a humid chamber overnight at room temperature. The following day, sections were washed in 1.0% NHS/PB, pH 7.4, and incubated in horse anti-goat immunoglobulin G (IgG; Vector Laboratories, Burlingame, CA) at a dilution of 25 μl/5 ml in 1.0% NHS/PB, pH 7.4, for 1–2 hours at room temperature. Next, sections were washed with PB and incubated in indocarbocyanine (Cy3)-conjugated streptavidin (Cy™3; Jackson ImmunoResearch Laboratories, Inc., West Grove, PA) in 0.01 M sodium phosphate buffer, pH 7.6, for 30–40 minutes. After washing through several changes of buffer, sections were coverslipped with Vector Shield (Vector Laboratories) and examined and photographed at a magnification of ×25 with a Leitz epifluorescence microscope (Leitz, Wetzlar, Germany).

### Control experiments

Several sections from each turtle eyecup were used for control experiments to test the specificity of the primary and secondary antibodies. Negative controls were performed by excluding the primary or secondary antibody from incubation according to the experimental paradigm described above.

### Quantitative data analysis

With the exception of S14–S16, for which only two animals were available, at least three turtles per stage were used for the quantification of ChAT-immunoreactive (-IR) cells and dendritic stratifications in the IPL. Analysis focused mainly in retinal regions at or near the visual streak. Photomicrographs (10.2 cm × 15.2 cm) of labeled regions were scanned with an Agfa StudioScan IIsi scanner (Agfa-Gevaert NV, Montsel, Belgium) at 29.5 pixels/cm and 256 gray levels. Data were obtained from these scans without consideration for tissue shrinkage, because the protocol used in this study minimized this factor. Cell density and dendritic strata positions were quantified by analyzing the scanned images with a program written in MatLab (MathWorks, Natick, MA) specifically for this study. The position and shape (curvature) of the proximal cholinergic dendritic stratum were deter-

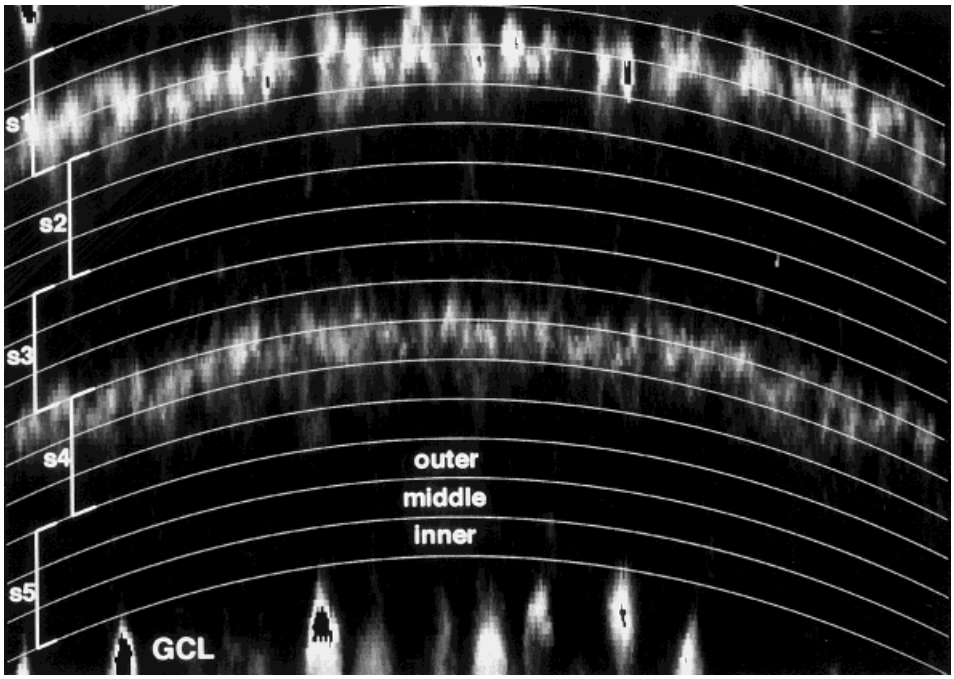


Fig. 1. Spatial layout of the quantitative analysis of a postnatal day 1 (P1) turtle inner plexiform layer (IPL). The IPL is grossly expanded in the vertical direction for demonstrating the positions of the IPL strata quantified by the equidistant polynomial lines. From distal to proximal, every three substrata denote outer, middle, and inner portions of a stratum. In the photomicrograph (53.7 μm × 250.2 μm), the distal choline acetyltransferase-immunoreactive (ChAT-IR) dendritic stratum is positioned near the middle and inner stratum (s1), and the proximal stratum is positioned near the s3–s4 border. ChAT-IR cells flank the IPL borders in the inner nuclear layer and the ganglion cell layer.

mined by placing three to five points on it, enabling Mathlab to find a polynomial fit (n points yielding a polynomial of order n-1). The position of the distal cholinergic stratum was then determined by placing a single point on it, because its shape typically was similar to that of the distal stratum. Next, the borders of the IPL were determined by placing single points where the IPL borders were judged to be located. On marking the borders of the IPL, MatLab separated the IPL into 15 equidistant zones with boundaries that had the shape of the proximal stratum (Fig. 1). Every three zones determined the outer, middle, or inner portion of a stratum, starting distally with s1 and ending proximally with s5. The intensity of labeling was integrated within each zone, and the 15 integrals were normalized such that the slightest immunoreactivity equaled 0, and the strongest immunoreactivity equaled 1. The means of these 15 values were then computed over the available sections at each stage. To determine the positions of the ChAT-IR dendritic strata as a function of developmental stage, the plot of the mean normalized labeling as a function of depth in the IPL was fitted with the sum of two Gaussian curves (Fig. 2). Their centers and standard deviations corresponded to positions and thicknesses of the dendritic strata. The relative positions of the dendritic stratifications were reported as the percentage of depth in the IPL with 0% located at the INL border and 100% located at the GCL border.

Next, the densities of ChAT-IR cells were estimated. A threshold for the intensities of immunoreactivity was defined at the 90-percentile mark. Cells were counted only if their pixels were continually above threshold for at least 5 μm [Guiloff and Kolb (1992) reported that the sizes of cholinergic amacrine cells ranged from 5 μm to 10 μm in diameter]. Because counts of cells may depend on the unknown correlation between the plane of section and their spatial distribution, the graphs of cell densities presented are not absolute but were normalized by the densities of ChAT-IR cells in the adult INL and GCL.

The statistical tests adopted for cell densities and dendritic positions always were nonparametric and robust (Sprent, 1993). To compare ChAT-IR densities between the INL and the GCL and the intensities of the distal and proximal dendritic stratifications, a two-sided Wilcoxon signed-rank test was used. Comparisons between measurements at two different stages were analyzed by using a one-sided Mann-Whitney test. The only exceptions were for the ratios of GCL densities versus INL densities and proximal and distal dendritic strata intensities, for which there were no a priori hypotheses, thus requiring two-sided tests. Trends in all of these measurements were tested with a one-sided Cox-Stuart test with the same exceptions cited above.

## RESULTS

Results for this study are grouped by developmental stages the under subheadings “Descriptive findings” and “Quantitative analysis.” The adult stage is reported first to establish a baseline with which other stages are compared.

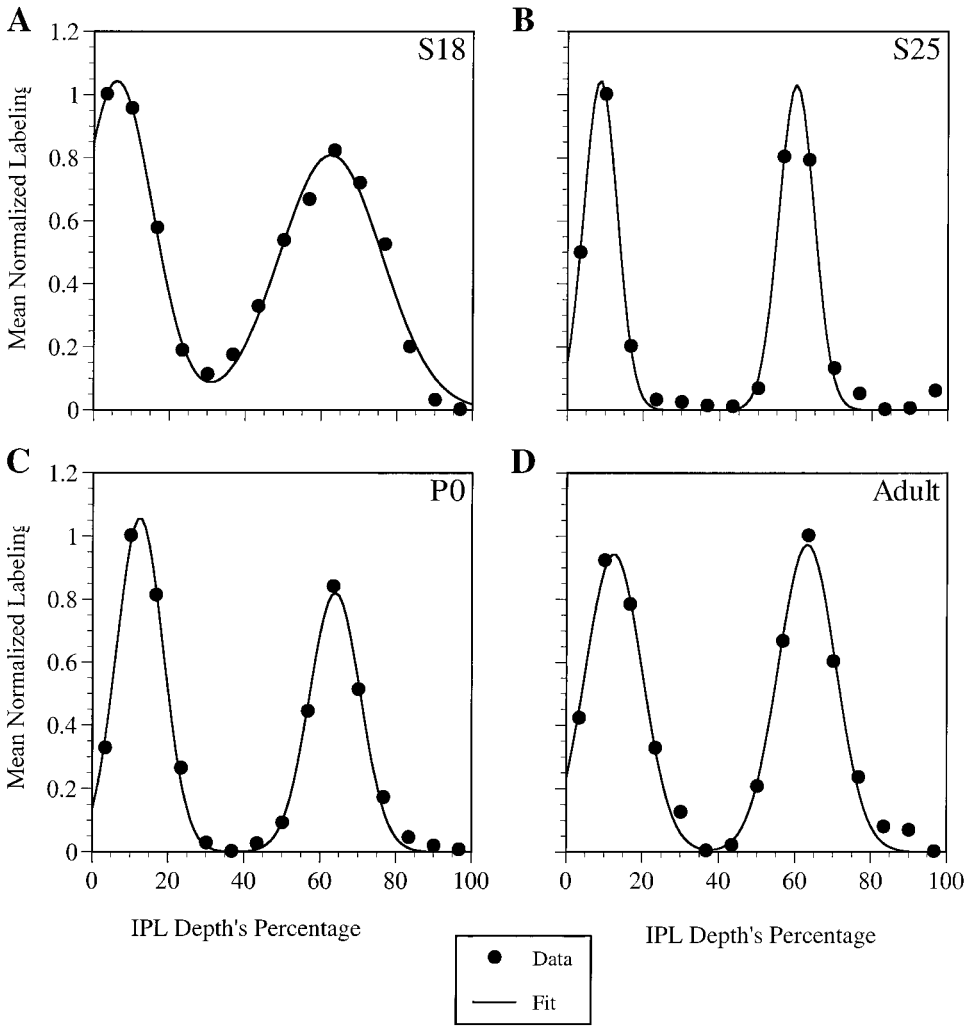


Fig. 2. **A–D:** Fits of the sum of two Gaussians to the labeling profile in the IPL from turtles at stage 18 (S18), S25, P0, and adult. The labeling intensity of each substratum in the IPL (15 in all; see Fig. 1) was integrated, and the values were normalized to the maximum, giving a bimodal distribution (solid dots). In other figures (see Figs. 10–12), the amplitudes, means, and standard deviations of the Gaussian fits are the intensities, positions, and thicknesses, respectively, of the ChAT-IR dendritic strata in the IPL. The closeness of the fits indicates that they are a good tool for quantifying the development of the ChAT-IR dendritic strata.

## Descriptive findings

***Adult.*** In the adult turtle retina (Fig. 3), ChAT-IR cells comprised two populations that were positioned on both sides of the IPL (Fig. 3A–C; see also Guiloff and Kolb, 1992). The morphology and regular spacing of these cells resembled the mirror-like symmetry of the starburst amacrine cells seen in mammals (Famiglietti, 1983a). Labeled dendritic processes from cholinergic amacrine cells in either the INL or the GCL often were seen to emanate from the immunoreactive cell bodies (Fig. 3D) and stratified either in the OFF sublamina or in the ON sublamina, respectively (Fig. 3C). The ChAT-IR dendritic stratification within the OFF sublamina appeared to have stronger immunoreactivity than that in the ON sublamina. A third type of ChAT-IR cells that resembled the type III cholinergic cells described by Guiloff and Kolb (1992) was observed occasionally in the middle of the INL (Fig. 3C, arrows). Labeling intensity was not always found to be weak for the type III ChAT-IR cells, as described in Guiloff and Kolb (1992). The sites of termination for these cells were not explored in the current study.

In the current study, ChAT antibodies did not label cell bodies in the outer nuclear layer (ONL) in the adult turtle retina, contrary to several previous reports (Lam, 1972; Schwartz and Bok, 1979). When a monoclonal antibody against ChAT (Boehringer Manneheim Corp., Indianapolis, IN) was used in a few pilot studies in the adult turtle retina (not reported in this study), this antibody labeled cells in the ONL indicative of photoreceptors. However, this monoclonal antibody did not result in sufficient labeling of cholinergic cells in the INL or GCL or sufficient dendritic stratifications in the IPL. Therefore, an affinity-purified polyclonal antibody from Chemicon (Temecula, CA) was used instead. Polyclonal antibodies have certain advantages over monoclonal antibodies. Polyclonal antibodies have higher affinities and wider reactivity for

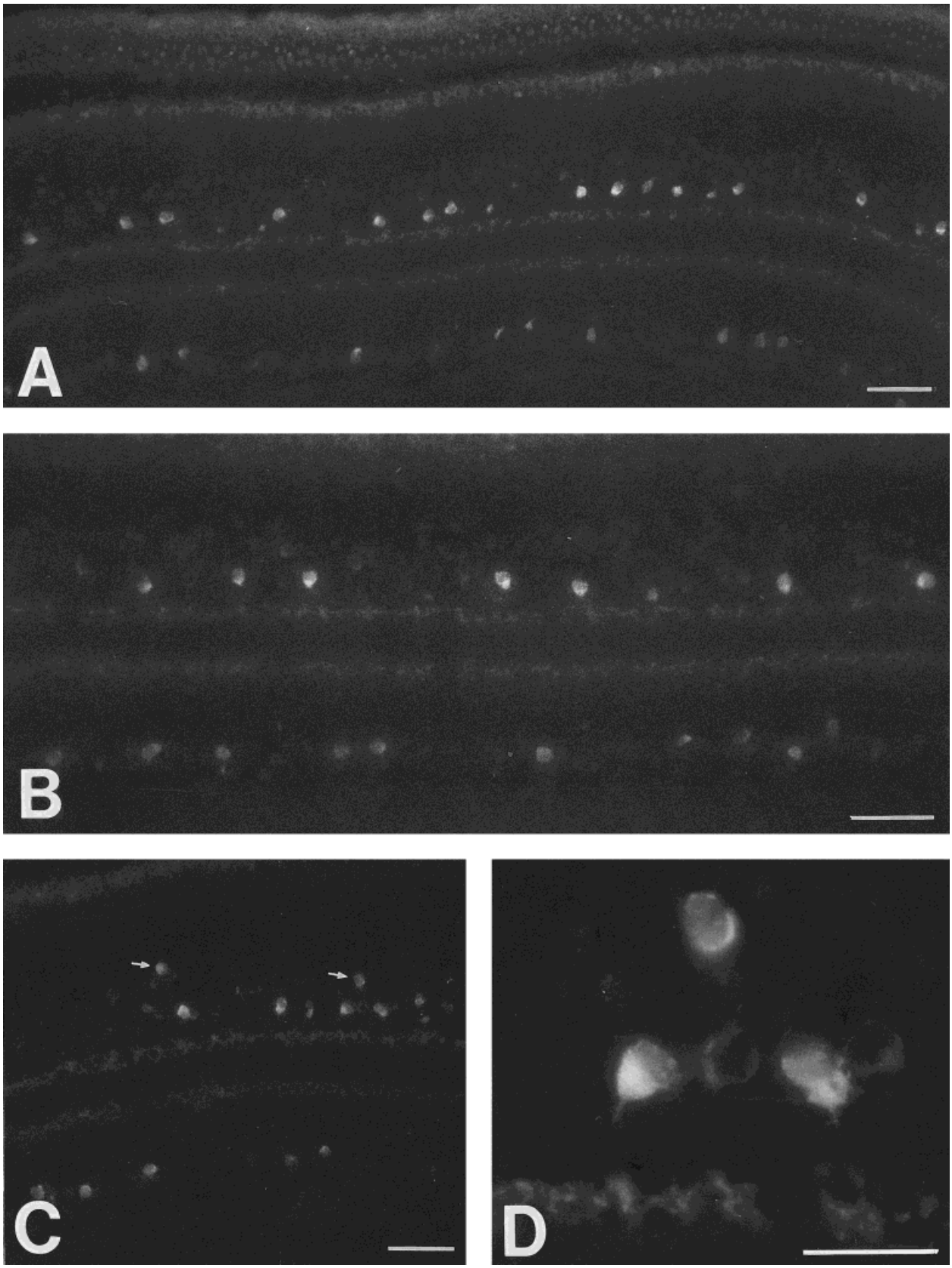


Fig. 3. **A–C:** Fluorescence photomicrographs of adult retinas demonstrating ChAT-labeled cells in the inner nuclear layer (INL), the ganglion cell layer (GCL), and the dendritic strata in the IPL (A–C, respectively). Labeled cells in the INL are slightly stronger in immunoreactivity than those in the GCL, and the distal dendritic stratum also is more fluorescent than the proximal dendritic stratum. In C, arrows indicate type III cholinergic cells that are positioned toward the middle of the INL. **D:** Higher magnification photomicrograph of one of the type III cholinergic cells shown in C. Scale bars = 50 μm in A–C; 20 μm in D.

epitopes, and they are more stable at different pH levels and salt concentrations (Beltz and Burd, 1989). In addition, turtles are cold-blooded vertebrates; thus, their retinas appear to be more immunoreactive to polyclonal antisera. The affinity-purified polyclonal antibody against ChAT was used because background labeling was greatly limited. The polyclonal antibody against ChAT used in the current study labeled regions around somata in the ONL, perhaps similar to the findings by Criswell and Brandon (1992), who reported labeling in axons and pedicles of turtle cone photoreceptors.

***S14–S16 (approximately E15–E22).*** The earliest stage obtained for this study, S14, revealed a retina with no subdivisions into the nuclear and plexiform layers. Faint immunoreactivity for ChAT was observed in areas near the vitreal surface (Fig. 4A). Immunoreactivity was not localized in cell bodies at this stage of development.

The retina at S15 also did not show nuclear or plexiform layers (Fig. 4B,C). At this stage, cells adjacent to the vitreal surface were ChAT immunoreactive; these cells had round to slightly oval shapes compared with the fusiform shape of the presumably neuroblastic cells that were located distally. Regions near the optic-nerve head had a high density of ChAT-IR cells, consisting of two to three rows of immunoreactive cells (Fig. 4B). In contrast, regions located farther from the optic nerve head comprised only one to two rows of immunoreactive cells (Fig. 4C).

At S16, the density of ChAT-IR cells remained high (Fig. 4D). Near the optic nerve head, the proximal half of the retina contained a groove indicative of a proto-IPL (Fig. 4D, arrow). The groove divided the ChAT-IR cells into two unequal populations, with the larger population in the proto-GCL and a single row of immunoreactive cells in the proto-INL. However, at regions of the retina located farther from the optic nerve head (not shown), development was less advanced, and the retina remained as an undivided layer, with ChAT-IR cells located near the vitreal surface. Compared with the adult retina shown in Figure 3, which consisted of a single row of ChAT-IR cells in the GCL, there appeared to be excess numbers of immunoreactive cells at these early stages.

***S18–S23 (approximately E25–E40).*** At S18, near the optic nerve head, the proto-IPL had developed into a definite IPL, which had separated the retina into a definitive GCL proximally and an INL distally (Fig. 5A). Within the IPL, two ChAT-IR dendritic strata with roughly equal fluorescence intensities were observed to ramify within the ON and OFF sublamina. From this early onset, these two dendritic stratifications remained relatively stable through adulthood. In the INL, the ChAT-IR cells formed a single row: Their spatial distribution was somewhat regular, and they had a polarity of immunolabeling directed toward the distal ChAT-IR dendritic stratum in the IPL. Comparatively, the ChAT-IR cells in the INL at S18 already resembled those in the adult retina. However, the ChAT-IR cells in the GCL continued to be as numerous as in the proto-GCL of the S16 retina.

By contrast, in regions located farther from the optic nerve head (Fig. 5B), development was less advanced at S18. The IPL in these regions still was forming, and ChAT-IR cells were still in the process of migration across the IPL. In these regions, ChAT-IR strata were not yet formed.

A thin, discontinuous line that was not immunolabeled appeared at S18 in the location of the future outer plexiform layer (OPL; Fig. 5A, arrow). Distal to this line, faint ChAT immunoreactivity was seen in some cells in the proto-ONL.

By S20, the process of cellular migration of ChAT-IR cells across the IPL appeared to have finished in all regions of the retina (Fig. 5C). At this stage, the retina consisted of three nuclear layers and two plexiform layers, as in the adult retina. A definitive OPL was present, and, in certain regions, photoreceptor cells were observed to be ChAT-IR. In terms of ChAT labeling, the retina appeared similar morphologically to the retina at S18 near the optic nerve head. These morphologic observations continued to S22 (not shown) and S23 (Fig. 5D).

***S25 (approximately E52).*** The retina at S25 (Fig. 6A,B) began to resemble the adult retina. In contrast to retinas at previous stages, the GCL at S25 contained significantly lower numbers of ChAT-IR cells. Furthermore, the presumptive displaced starburst amacrine cells appeared brighter against the rest of the cells, which showed faint immunoreactivity. In the INL, immunoreactive cells continued to form a single layer, and, together, the cholinergic populations of the INL and the GCL formed a mirror-like symmetry. The brightly labeled cells on both sides of the IPL were round to slightly oval in morphology and had a polarity that was directed toward their respective immunoreactive strata in the IPL.

At this stage, the type III ChAT-IR cells (Guiloff and Kolb, 1992), which were located toward the middle of the INL, made their appearance in the retina (Fig. 6C). These cells were not round and homogenous, and they were not distributed at the regular intervals seen in the adult-like cholinergic cells, which were positioned at the INL/IPL border.

***Birth to postnatal day 28.*** At birth [postnatal day (0)], two populations of ChAT-IR cells were situated close to the IPL borders, forming a mirror-like symmetry pattern similar to the adult retina. The high density of ChAT-IR cells present in the GCL during early embryonic stages was greatly reduced or absent at birth. In the IPL, the two immunoreactive dendritic strata had different fluorescence intensities, similar to the adult retina but different from the previous stages. The distal dendritic stratum was observed to be more strongly immunoreactive than the proximal dendritic stratum.

At P1, however, the morphology of the retinas with respect to ChAT immunoreactivity was variable. In Figure 6C, the retina resembles retinas at S25 (Fig. 6A,B) and in adults (Fig. 3). However, in Figure 6D, a higher density of ChAT-IR cells reappears in the GCL. The reason for their "return" is unknown, although it may have been due to one or more of three reasons: First, at P1, the retina had been exposed recently to light, and cells may have reacted to this at some biochemical level. Second, the process of birth may have caused dramatic hormonal changes that could affect the cells (Hoskins, 1990; Negishi and Wagner, 1995; Gorovits et al., 1996). Finally, the turtle is a cold-blooded vertebrate; therefore, factors such as fluctuations in ambient temperature could affect the rate of development. Therefore, although both photomicrographs in Figure 6C,D were obtained from P1 retinas, they may have differed developmentally from one another. A rare observation of a ChAT-IR cell was made in the IPL (Fig. 6D): Its functional significance is not known. Labeling for ChAT in

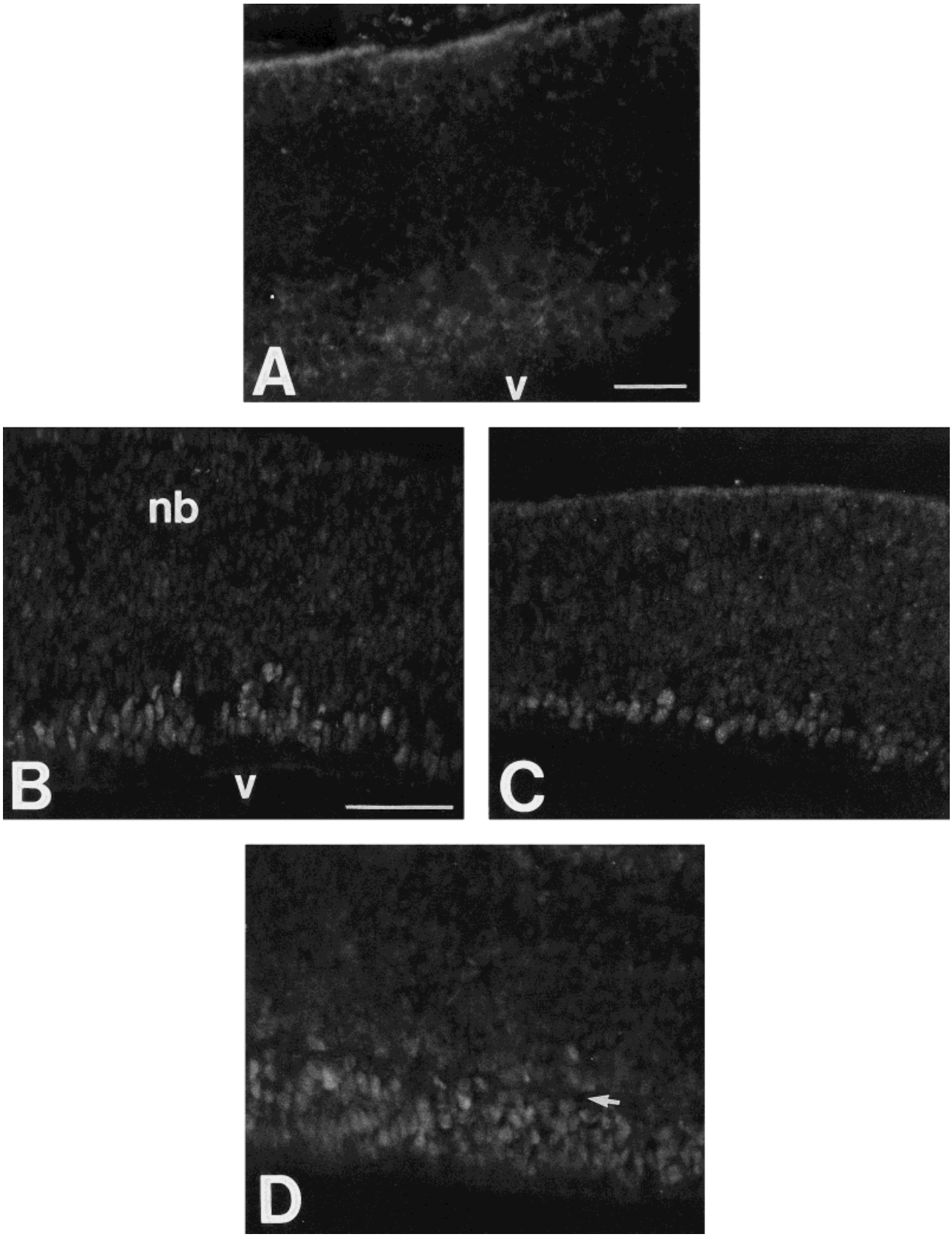


Fig. 4. Fluorescence photomicrographs of S14–S16 retinas demonstrating early localization of ChAT. **A:** At S14, the retina has no subdivisions into the nuclear and plexiform layers, with slight immunoreactivity near the vitreal (v) surface. **B,C:** At S15, the retina still does not have subdivisions, and ChAT-IR cells are located near the vitreal surface; these cells are morphologically distinct from the neuroblastic (nb) cells that are located distially. Development is more advanced near the optic-nerve head (B) than in a region farther away (C). **D:** At S16, the retina has grown and contains increasingly greater numbers ChAT-IR cells near the vitreal surface. A proto-IPL is indicated by a groove (arrow). Scale bars = 50 μm in A; 50 μm in B–D.

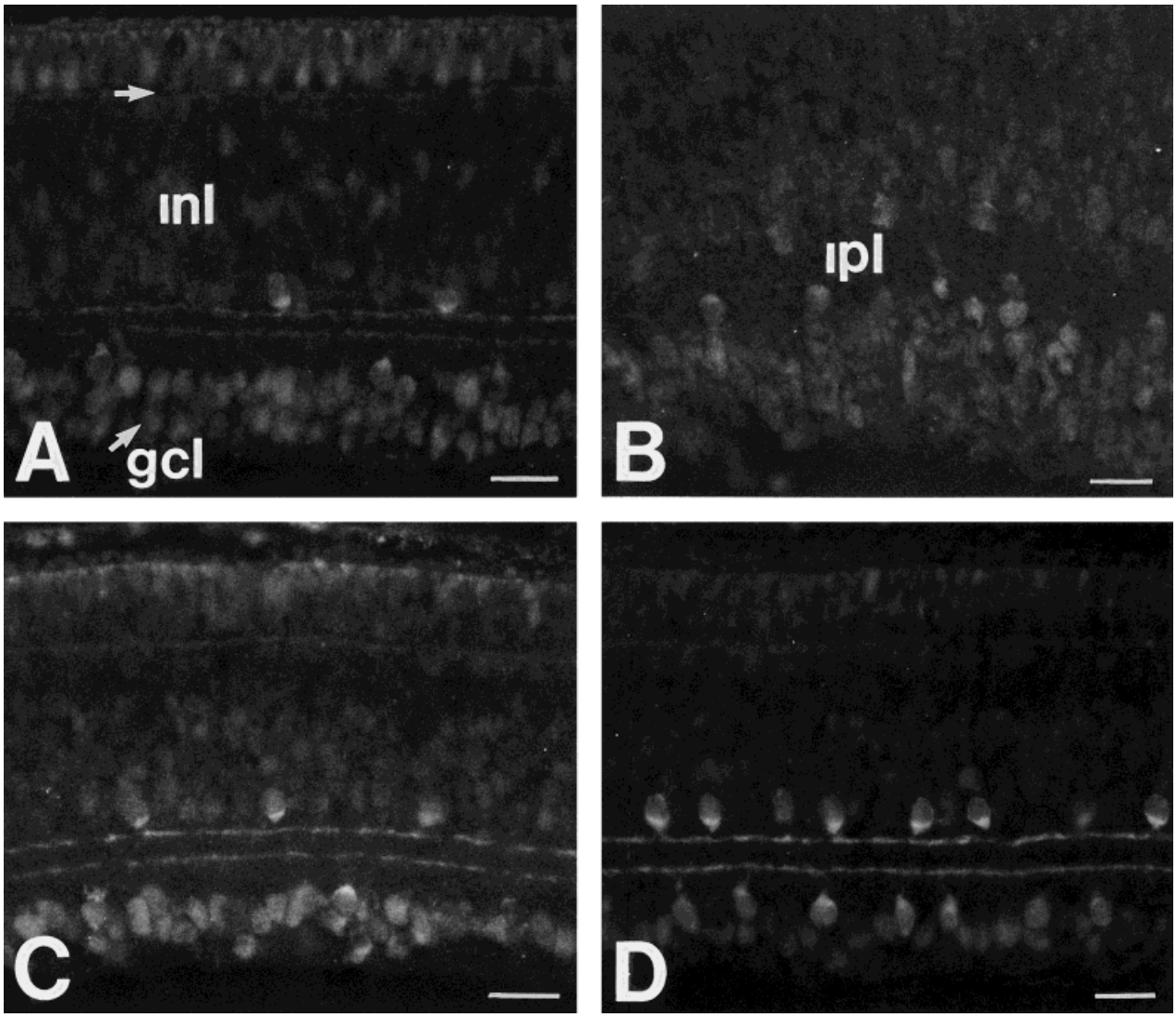


Fig. 5. Fluorescence photomicrographs of S18–S23 retinas demonstrating ChAT-IR cells and the formation of ChAT-labeled dendritic strata in the IPL. **A,B:** At S18, near the optic nerve head (A), the IPL is formed, and ChAT-IR dendritic strata are present. ChAT-IR cells appear in the INL and the GCL, with a high density of labeled cells in the latter region. The horizontal arrow denotes the presence of the outer plexiform layer (OPL) at this early stage. Distal to the OPL, several cells are ChAT-IR: These cells represent ChAT-IR photoreceptors. Farther from the optic nerve head (B), the IPL still is forming, and ChAT-IR cells are in the process of migration across the IPL. **C:** At S20, the retina is not much different from that shown in A with respect to ChAT immunoreactivity. **D:** At S23, ChAT-IR cells are located in the INL and the GCL, and the labeled dendritic strata are located in the IPL in relatively the same position as at S20. Scale bars = 20 μm.

retinas from P7 (Fig. 6E) to P28 (not shown) resembled that seen in the adult retinas.

## Quantitative Analysis

The morphology of the adult turtle retina, as described above, was different from the developing retina not only in terms of size and layers but also in terms of the number of cells that contained ChAT. It was seen that the developing retina contained more ChAT-IR cells than the postnatal and adult retina. To follow the variation in the density of ChAT-IR cells as a function of age, the density was normalized to the adult values for the GCL and the INL and is charted in Figure 7.

Whereas the density of ChAT-IR cells in the GCL declined with development, the density in the INL was relatively constant from S16 to adulthood. The downward trend observed in the GCL was statistically significant ($P < 0.016$); this trend began after S18 and was completed by P7. At S16 and S18, the GCL densities were about four times greater than that of the adult. These declines in the GCL densities were not smooth, displaying two small but statistically significant fluctuations at S22 and P1 ($P < 0.01$ and $P < 0.001$, respectively). At S20, the density of ChAT-IR cells in the GCL had declined to 1.8 times the adult density, but it increased slightly to 2.5 times the adult value at S22. At birth, the relative density of labeled

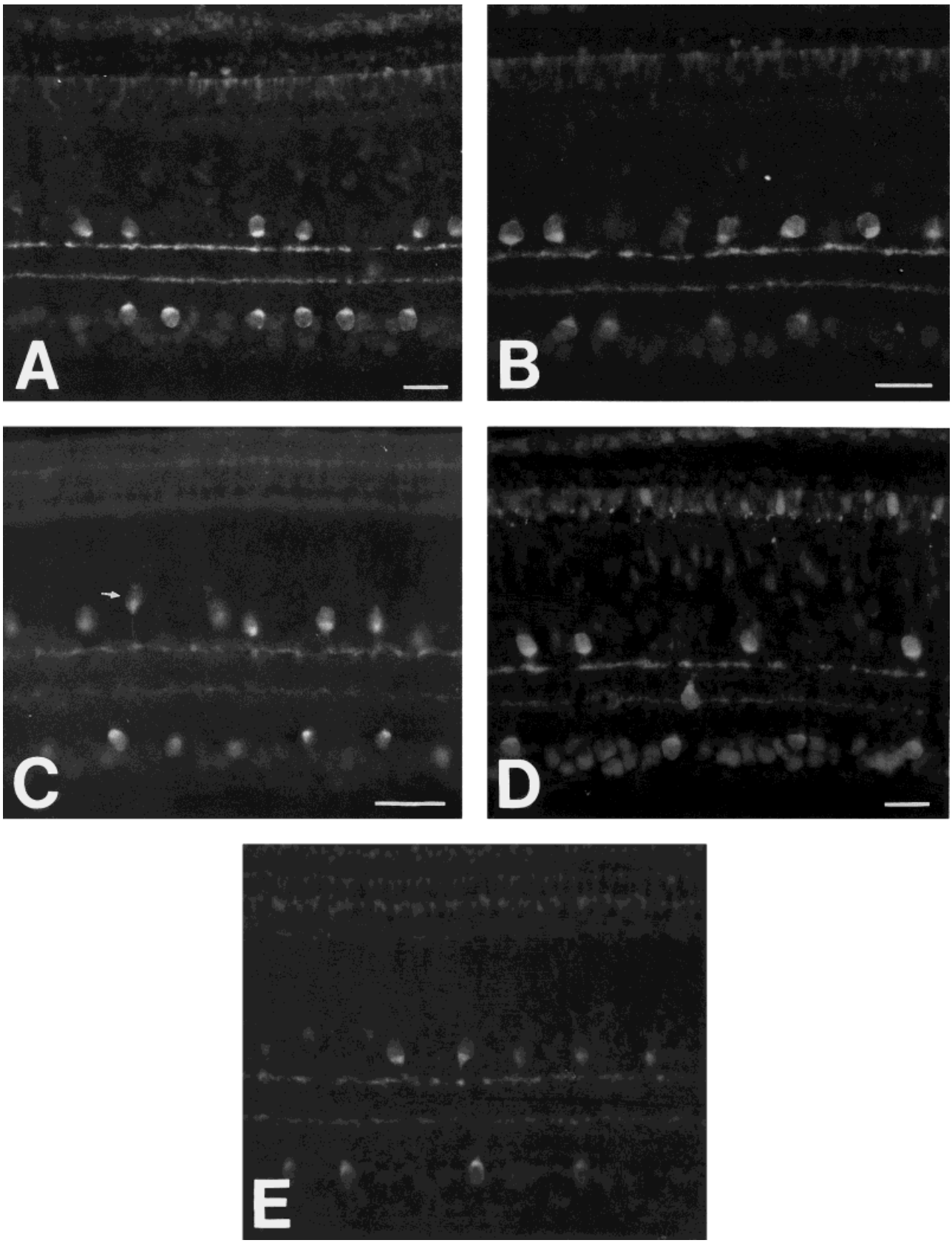


Fig. 6. Fluorescence photomicrographs of S25–P7 retinas demonstrating the adult-like cholinergic amacrine cells. **A,B:** At S25, ChAT-IR cells are distributed on both sides of the IPL in a fashion similar to the adult retina. The distal ChAT-IR dendritic stratum is slightly more immunoreactive than the proximal dendritic stratum. **C,D:** At P1, the retinas do not display similar ChAT morphology from animal to animal. In C, the retina is similar to S25; however, in D, the high density of ChAT-IR cells that has diminished since S23 is present again in the GCL. In addition, several cells in the outer nuclear layer (ONL) are labeled for ChAT. The arrow in C indicates a type III cholinergic cell, and a rare labeled cell in the IPL in D is unknown. **E:** By P7, the morphology of the retina with respect to its immunoreactivity to ChAT resembles the adult form again. Scale bars = 20 μm in A,B; 30 μm in C; 20 μm in D–E.

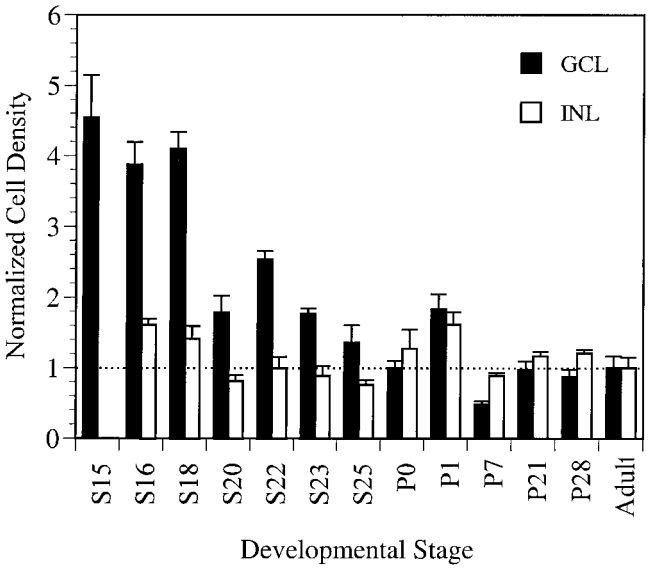


Fig. 7. Histogram of the density of ChAT-IR cells in the GCL and the INL as a function of developmental stage. All values for the different developmental stages were normalized to the adult value, which was set at 1. The overall trend in this graph demonstrates that the density of cells in the GCL is high early in development and diminishes with subsequent stages. The density of cells that are ChAT-IR in the INL, however, is relatively stable from early in development.

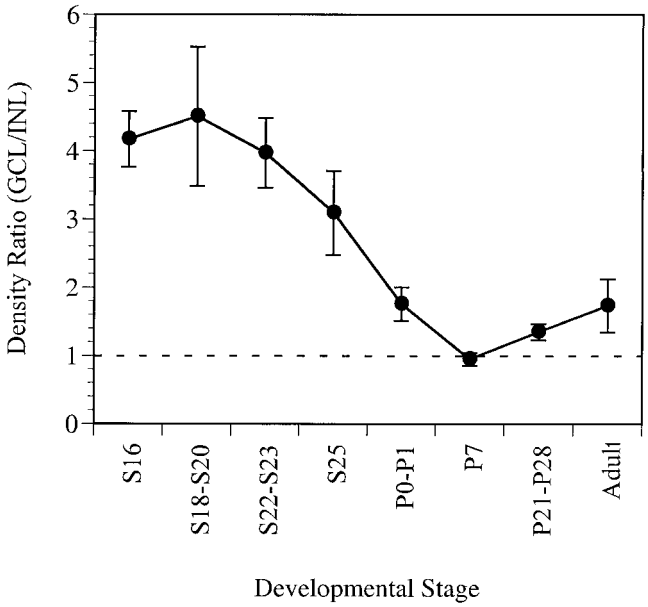


Fig. 8. Ratio between the densities of ChAT-IR cells in the GCL versus the INL as a function of developmental stage. This ratio is approximately 4 early in development and declines smoothly as a function of age, becoming close to 1 at around P7. After P7, the ratio rises slightly, reaching 1.7 for the adult retina.

cells in the GCL was slightly under 1.0, but it increased to 1.8 at P1. After P1, and particular after P21, the relative ChAT-IR density in the GCL appeared to stabilize to the adult value.

Because the density of ChAT-IR cells in the GCL declined, whereas their density in the INL remained fairly constant, their ratio also declined with development (Fig. 8). The downward trend of this ratio as a function of age was statistically significant ($P < 0.016$). At P7, however, the ratio was near 1.0, and it increased slightly to the adult value ($P < 0.05$). There were more than four times more ChAT-IR cells in the GCL than in the INL from S16 to S20. By contrast, in the adult retina, the ratio of the density of labeled cells in the GCL versus the INL was approximately 1.7. Elsewhere, a slightly greater ratio of cholinergic cells has been demonstrated in adult mammals (Vaney et al., 1981; Famiglietti and Tumosa, 1987).

## ChAT-IR strata in the IPL

In the adult retina (Fig. 3) and at other developmental stages, two distinct ChAT-IR dendritic strata were visible in the IPL. Figure 9 shows how the ChAT labeling in the IPL was distributed at different developmental stages. These ChAT-IR strata always were observed in relatively similar positions from S18 to adulthood. The distal dendritic stratum was situated near the s1–s2 border, and the proximal dendritic stratum was situated near the s3–s4 border. The dendritic strata positions were observed to be relatively constant as early as S18 despite the growth of the IPL during development.

However, closer examination revealed that the positions of these dendritic strata, as relative percentages of IPL depth, varied slightly with age (Fig. 10). The trends for the outer (distal) and inner (proximal) dendritic strata were of statistically significant shifts toward more proximal ($P < 0.032$) and distal ($P < 0.032$) positions, respectively. From S18 to S25, the distal dendritic stratum shifted from 6% to 11.7%. After S25, the distal stratum showed only small shifts to more proximal positions and appeared to be stabilizing at its position in the adult. In contrast, at around the time of birth, the proximal stratum showed a sudden shift, albeit small, from 61.8% to a more distal position around 58.1% of the IPL depth. Otherwise, the position of the proximal dendritic stratum was stable except for minor fluctuations. In the adult retina, this position was measured at approximately 57.1% of the IPL depth.

In addition to the changes in dendritic strata position, it was observed that the ChAT-IR dendritic strata thicknesses also changed with development. Figure 11 shows that both the distal and proximal strata began with thick spreads and decreased with development. This trend in spread was statistically significant for the outer dendritic stratum ($P < 0.032$) but not for the inner dendritic stratum. An important exception to this trend occurred between P28 and adulthood: During this period, the distal and proximal dendritic strata thickened from 4.5% and 4.8% of the IPL to 6.4% and 6.8%, respectively.

A final developmental trend worth mentioning occurred in the intensity of labeling of the dendritic strata (Fig. 12). The distal and proximal dendritic strata were observed to have similar fluorescence intensity during the embryonic stages. However, around the time of birth and with subsequent stages to adulthood, the labeling ratio between the distal and proximal strata increased by a factor of approximately 1.5. This trend in labeling ratio was statistically significant ($P < 0.032$).

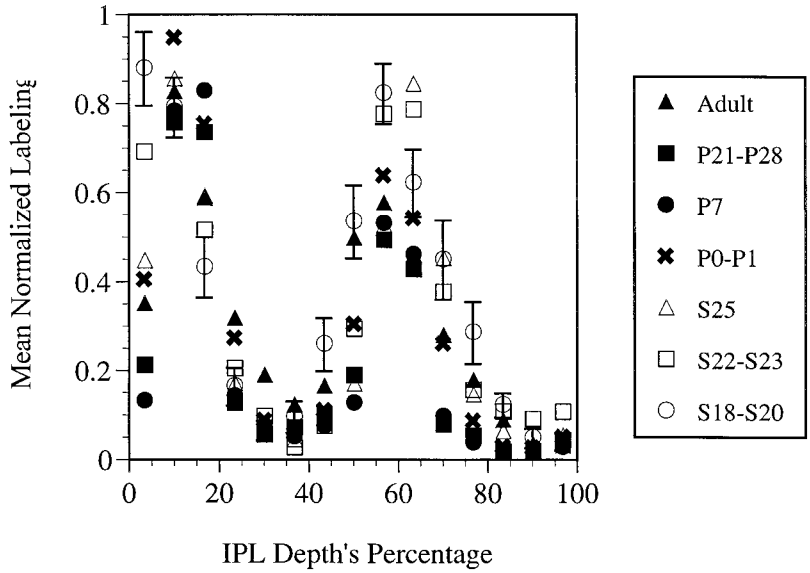


Fig. 9. Spatial distribution of ChAT immunoreactivity in the IPL parametric on developmental stages. The spatial position in this graph is quantified as a percentage of depth in the IPL. The vertical lines divide the graph into five equidistant strata (s1–s5). One set of representative error bars (S18–S20) was depicted to simplify the figure. ChAT-IR dendritic strata, indicated by the graph's bimodal distribution, are shown to be relatively stable from their appearance in the IPL at S18 to adulthood.

## DISCUSSION

In the current study, the developmental patterns of cells that were ChAT-IR were investigated in the turtle retina from S14 to adulthood. The findings in this study demonstrate that cells are ChAT-IR early in development and that this population includes the presumed starburst amacrine cells. Support for the early localization of ChAT prior to synaptogenesis in the developing embryonic vertebrate retina comes from data in retinas of the chick (Spira et al., 1987) and *Xenopus* (Ma and Grant, 1978). However, this is the first study to describe not only the pattern of development of cells expressing ChAT but also to present compelling evidence that cells other than the presumed starburst amacrine cells transiently express ChAT early in development.

### Appearance and development of ChAT in the INL and GCL

Development and maturation in the turtle retina follows a spatiotemporal gradient from areas near the optic nerve head to regions farther away, as in development of the ferret retina (Reese et al., 1994). The anatomy of the turtle retina when ChAT is observed first localizing in cells, at S15, is similar to that of the chick retina (Spira et al., 1987). At this stage, the retina has no subdivisions into nuclear and plexiform layers and consists mainly of undifferentiated, neuroblastic cells. Proximally, there are one or two rows of cells that are ChAT-IR. In regions near the optic nerve head and as early as S16, the formation of the IPL separates ChAT-IR cells into two populations, and a high density of labeled cells is observed in the proto-GCL. This contrasts with the adult retina, in which only small percentages of cells in the GCL are ChAT-IR. Therefore, in the current study, cells that are ChAT-IR may include not only the adult-like cholinergic amacrine cells but also another unidentified population. The reason for the excess numbers of cells that express ChAT in the developing retina and that, therefore, probably are cholinergic in function, can only be speculated. Acetylcholine is has been found in migrating crest cells (Smith et al., 1979), and, in 8-day-old chick retina, it stimulates platelet-activating factor, which, in turn, mediates cellular differentiation (Bussolino et al., 1988). Furthermore, acetylcholine may act at muscarinic receptors early in development for neurogenesis and cell migration (Redburn and Rowe-Rendleman, 1996). Later, differentiation is regulated at nicotinic receptors (Wong, 1995). However, at the level of electron microscopy, the IPL of turtle retinas younger than S20 shows very little membrane appositions and no synaptic vesicles (De Juan et al., 1996). Hence, acetylcholine at these early stages does not appear to function through conventional synapses.

By S18, in regions of the retina near the optic nerve head, where development is more advanced, the borders between the cellular (INL and GCL) and dendritic (IPL) layers are established. In these instances, the ChAT-IR cells in the INL display morphology and regular spacing (Vaney et al., 1981) that bears a striking resemblance to the adult cholinergic amacrine cells. In addition, the resemblance extends to the dendritic stratification (Guiloff and Kolb, 1992). Therefore, adult-like cholinergic amacrine cells in the INL make their appearance early and are relatively stable throughout development.

By contrast, in the GCL, at the time of the appearance and establishment of the IPL (S16–S18), the density of ChAT-IR cells is high. After S18, however, the density declines, and, in the adult retina, the ratio of ChAT-IR cells in the GCL versus the INL is about 1.7. This ratio is in agreement with the observation in mammals that the number of displaced cholinergic amacrines is slightly higher than those in the INL (Vaney et al., 1981; Famiglietti and Tumosa, 1987).

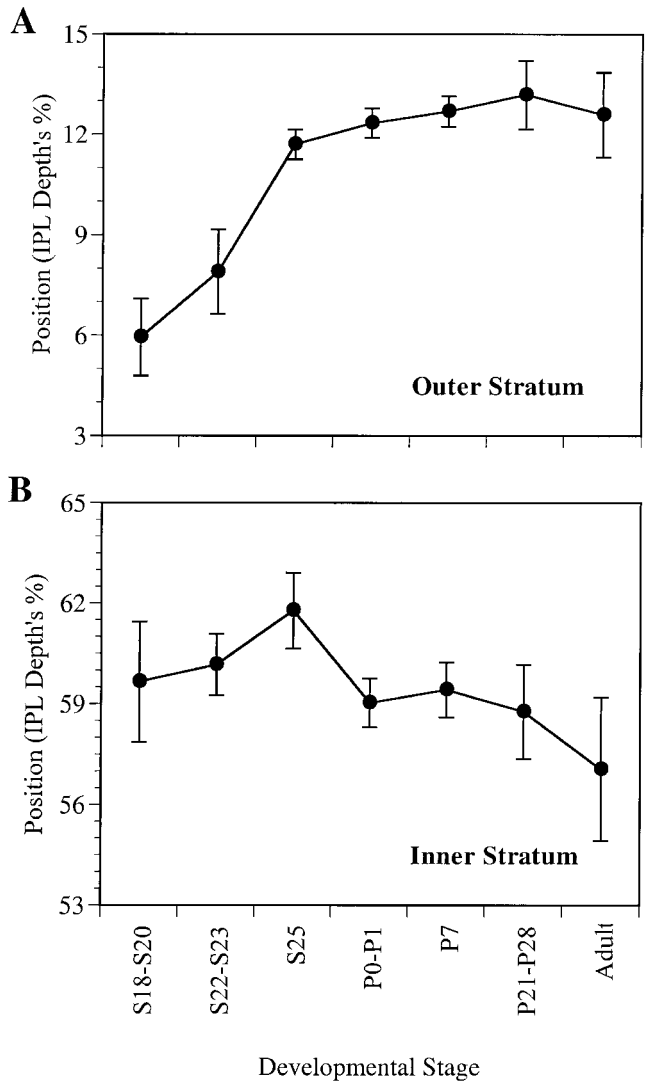


Fig. 10. Position of the distal (outer) and proximal (inner) ChAT-IR dendritic strata as a function of developmental stage. The unit of position is expressed as the percentage of depth in the IPL. Compared with the positions of the adult ChAT-IR strata, the two strata are located closer to their cell bodies early in development. The distal stratum shifts to a more proximal position with development, stabilizes around S25, and remains stable thereafter. The proximal stratum has an abrupt shift to a more distal position between S25 and P0 then shifts back distally around birth.

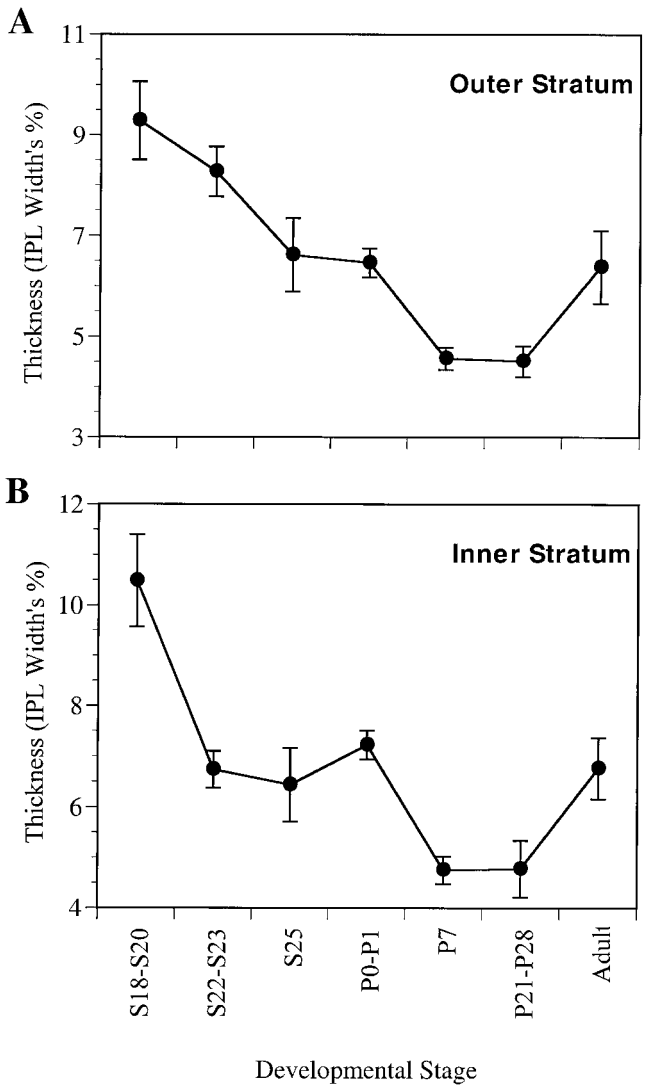


Fig. 11. Thickness of the distal (outer) and proximal (inner) ChAT-IR dendritic strata as a function of developmental stage. The unit of thickness is expressed as the percentage of IPL thickness. The overall trend of these graphs is that, early in development, the ChAT-IR dendritic strata appear thick in the IPL and then narrow down with age.

The adult-like, displaced cholinergic amacrine cells are likely to be in place in the GCL early in development, perhaps as early as S18, or even at S16 in the proto-GCL (see the accompanying paper: Nguyen and Grzywacz, 2000). This assumption is strengthened by the appearance of the proximal ChAT-IR dendritic stratification at S18. Therefore, like the cholinergic population that resides in the INL, this displaced cholinergic population is most likely to be present early in development but is "camouflaged" among the rest of the ChAT-IR cells in the GCL. With the decline and disappearance of the ChAT-IR transient population at subsequent stages, the adult-like cholinergic amacrine cells in the GCL are observed clearly.

The type III cholinergic cells were observed relatively late in development, from S25 to adulthood, and this confirmed findings in the chicken (Baughman and Bader, 1977; Millar et al., 1987; Spira et al., 1987) and adult turtle (Guiloff and Kolb, 1992) retinas. These type III cholinergic cells have been noted to be less prominent in the turtle than in the chicken retina (Guiloff and Kolb, 1992). However, in the current study, the staining intensity of these type III cholinergic cells was not always faint, as reported previously by Guiloff and Kolb (1992). Differences in the labeling pattern may be attributable to the methodology or antibodies used. The dendritic stratification of these cells could not be determined in the current study, although they have been described to have bistratifications or tristratifications in the IPL (Guiloff and Kolb, 1992). The significance of these cells is not known.

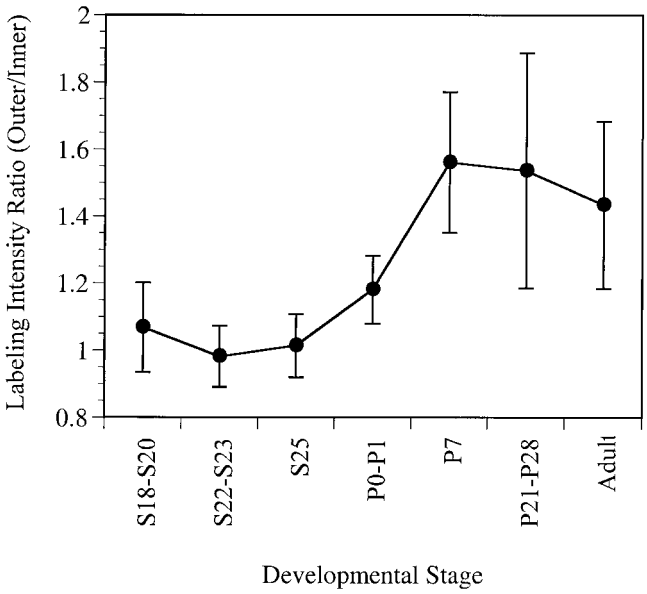


Fig. 12. Labeling intensity ratio of distal (outer) versus proximal (inner) ChAT-IR dendritic strata as a function of developmental stage. This ratio increases with age, with a particularly sharp rise between S25 and P0. Only during embryogenesis are the proximal and distal labeling intensities similar.

An important component of the cholinergic system is acetylcholinesterase (AChE). This hydrolyzing enzyme of acetylcholine also has been found to be expressed early during the development of the chick retina (Spira et al., 1987; Layer, 1991; Reiss et al., 1996; Layer et al., 1997). The expression of AChE was not explored in the current study; however, in the chick retina, the expression of AChE appears before ChAT (Spira et al., 1987; Reiss et al., 1996), before synaptogenesis, and apparently well before ON-OFF channels are formed in the IPL (Layer, 1991; Layer et al., 1997). AChE is involved in cellular migration (Layer, 1991; for review, see Layer and Willbold, 1994) and differentiation (Layer et al., 1988; Layer, 1991; Robitzki et al., 1997; for reviews, see Layer and Willbold, 1994; Small et al., 1996). Furthermore, mounting evidence indicates that AChE may play a role in cellular adhesion, supporting neurite outgrowth (Layer et al., 1993; for reviews, see Layer and Willbold, 1994; Small et al., 1996). In light of these findings, early in retinal development, acetylcholine and AChE have morphogenic roles that are unrelated to their neurotransmission.

## Relative position and thickness of ChAT-IR dendritic stratifications in the IPL

In the adult retina, the relative position of the proximal cholinergic dendritic stratum is similar to the findings by Criswell and Brandon (1992), but the position of the distal dendritic stratum in the current study differs slightly from theirs. Those authors reported that the distal stratum ranged from 16% to 21% of the IPL depth, whereas it was found at approximately 13% of the IPL depth in the current study.

As early as S18, Two ChAT-IR dendritic strata are observed as early as S18 near the optic nerve head, where development is more advanced, and the IPL is observed as a distinct layer. The proximal ChAT-IR stratum appears to be close to the adult position early in development, undergoing a small but significant shift to a more distal position with age. In contrast, the position of the distal ChAT-IR dendritic stratum is observed to increase twofold with development, shifting to a more proximal position (Fig. 10). These shifts are inconsistent with the hypothesis that development homogeneously adds a net amount of dendrites and axons throughout the IPL. This hypothesis would predict that the relative positions of the cholinergic dendritic stratifications should remain constant. An alternative hypothesis is that new dendrites and axons are added preferentially near the IPL borders. Such additions would cause the cholinergic stratifications to be relatively closer to the middle of the IPL, as observed in Figure 10. Furthermore, this hypothesis accounts for the relatively greater shift of the distal cholinergic stratification compared with that of the proximal stratification, because the former is closer to the IPL border to begin with and, thus, has farther to go. Finally, the hypothesis also is consistent with the relative thinning of the stratifications with age (Fig. 11).

The ChAT-IR dendritic stratifications are observed in the IPL as early as S18. Because synaptogenesis does not occur until at least S22 in the turtle (De Juan et al., 1996), approximately 10 days after the appearance of the strata, they are being laid down before synaptogenesis. This, coupled with their relatively precise and stable positions in the IPL, suggests that the cholinergic dendritic strata may serve as beacons to certain growing neurites in the early retina. It is noted that, in the developing chick retina, AChE-IR strata are present earlier than ChAT-IR strata in the ON and OFF sublamina (Reiss et al., 1996; Layer et al., 1997). Hence, AChE strata also may work as beacons to neurites, at least in the chick retina. In addition, data from chick and turtle retinas regarding acetylcholine and AChE can be interpreted to show that the ON and OFF channels do not require conventional synaptic (electrical) activity early in development.

## ChAT immunoreactivity in photoreceptor cells

ChAT immunoreactivity is found in turtle photoreceptor cells as early as S18, in agreement with other studies in adult turtle retina (Lam, 1972; Criswell and Brandon, 1992) and in goldfish retina (Schwartz and Bok, 1979). In the rabbit retina, Masland and Mills (1979) demonstrated that photoreceptors synthesize a significant amount of choline-containing phospholipids, possibly related to the high membrane turnover in these cells. However, in the turtle retina, photoreceptors appear to uptake choline not just due to high membrane turnover but perhaps also to produce acetylcholine, as evidence by their expression of ChAT (Criswell and Brandon, 1992). In this study, ChAT immunoreactivity in photoreceptors was localized in the cell body during early stages (S18–S25), and labeling became less frequent at later stages. In the adult retina, ChAT does not appear to be localized in cell bodies but, instead, perhaps is localized to pedicles and axon terminals (Criswell and Brandon, 1992). It is not known whether the localization of ChAT in cell bodies of photoreceptors during the embryonic stages indicates a transmitter function. At least in the mammalian adult retina, such function is highly unlikely (Massey and Redburn, 1987). In contrast, during neonatal life, a chronic applica-

tion of curare to turtle retinas causes losses in outer-segment discs and alteration in nuclei at the outer and inner nuclear layers (Guardiola et al., 1997). This suggests that acetylcholine acts through nicotinic receptors and may control high-affinity uptake of choline, at least by photoreceptors.

## CONCLUSIONS

Cells in the turtle retina express ChAT early in development. These cells comprise the presumed starburst amacrine cells that reside in the INL and the GCL and a population in the GCL that transiently expresses ChAT. The presumed starburst amacrine cells establish their positions on both borders of the IPL, and their dendritic strata are observed within the IPL prior to synaptogenesis and the emergence of any electrical activity in the retina. The population that transiently expresses ChAT declines with development and disappears around birth. The functional significance of this "transient" cholinergic population in the GCL is not known; however, in the accompanying paper (Nguyen and Grzywacz, 2000), it is demonstrated that the adult-like, displaced cholinergic amacrine cell population is not a subset of this transient cholinergic population.

## ACKNOWLEDGMENTS

This work was also supported by a National Eye Institute core grant to the Smith-Kettlewell Eye Research Institute, and by the William A. Kettlewell Chair (N.M.G.). The authors thank David Merwine for his assistance in the removal of the eye cups and Kliebert (Hammond, LA) for their timely delivery of the turtle eggs.

## LITERATURE CITED

Ariel M, Daw NW. 1982. Pharmacological analysis of directionally sensitive rabbit retinal ganglion cells. J Physiol (Lond) 324:161–185.

Baughman RW, Bader CR. 1977. Biochemical characterization and cellular localization of the cholinergic system in the chicken retina. Brain Res 138:469–485.

Beltz BS, Burd GD. 1989. Overview of immunocytochemical techniques. In: Immunocytochemical techniques: principles and practice. Cambridge: Blackwell Scientific Publications, Inc. p 19–28.

Brandon C. 1991. Cholinergic amacrine neurons of the dogfish retina. Vis Neurosci 6:553–562.

Bussolino F, Pescarmona G, Camussi G, Gremo F. 1988. Acetylcholine and dopamine promote the production of platelet activating factor in immature cells of chick embryonic retina. J Neurochem 51:1755–1759.

Catsicas M, Bonness V, Becker D, Mobbs P. 1998. Spontaneous Ca2+ transients and their transmission in the developing chick retina. Curr Biol 8:283–286.

Conley M, Fitzpatrick D, Lachica EA. 1986. Laminar asymmetry in the distribution of choline acetyltransferase-immunoreactive neurons in the retina of the tree shrew (*Tupaia belangeri*). Brain Res 399:332–338.

Copenhagen DR. 1996. Retinal development: on the crest of an exciting wave. Curr Biol 6:1368–1370.

Criswell MH, Brandon C. 1992. Cholinergic and GABAergic neurons occur in both the distal and proximal turtle retina. Brain Res 577:101–111.

Dann JF. 1989. Cholinergic amacrine cells in the developing cat retina. J Comp Neurol 289:143–155.

De Juan J, Grzywacz NM, Guardiola JV, Sernagor E. 1996. Coincidence of synaptogenesis and emergence of spontaneous and light-evoked activity in embryonic turtle retina. ARVO Abstr 37:634.

Eckenstein F, Thoenen H. 1982. Production of specific antisera and monoclonal antibodies to choline acetyltransferase: characterization and use for identification of cholinergic neurons. EMBO J 1:363–368.

Famiglietti EVJ. 1983a. "Starburst" amacrine cells and cholinergic neurons: mirror-symmetric on and off amacrine cells of rabbit retina. Brain Res 261:138–144.

Famiglietti EVJ. 1983b. On and off pathways through amacrine cells in mammalian retina: the synaptic connections of "starburst" amacrine cells. Vision Res 23:1265–1279.

Famiglietti EV. 1987. Starburst amacrine cells in cat retina are associated with bistratified, presumed directionally selective, ganglion cells. Brain Res 413:404–408.

Famiglietti EV. 1992. Dendritic co-stratification of ON and ON-OFF directionally selective ganglion cells with starburst amacrine cells in rabbit retina. J Comp Neurol 324:322–335.

Famiglietti EV, Tumosa N. 1987. Immunocytochemical staining of cholinergic amacrine cells in rabbit retina. Brain Res 413:398–403.

Feller MB, Wellis DP, Stellwagen D, Werblin FS, Shatz CJ. 1996. Requirement for cholinergic synaptic transmission in the propagation of spontaneous retinal waves. Science 272:1182–1187.

Galli L, Maffei L. 1988. Spontaneous impulse activity of rat retinal ganglion cells in prenatal life. Science 242:90–91.

Gorovits R, Yakir A, Fox LE, Vardimon L. 1996. Hormonal and non-hormonal regulation of glutamine synthetase in the developing neural retina. Brain Res Mol Brain Res 43:321–329.

Grzywacz NM, Amthor FR, Merwine DK. 1998. Necessity of acetylcholine for retinal directionally selective responses to drifting gratings in rabbit. J Physiol (Lond) 512:575–581.

Guardiola JV, Sernagor E, De Juan J, Grzywacz NM. 1997. Histological changes in turtles' neonatal retinas by nicotinic blockade. ARVO Abstr.

Guiloff GD, Kolb H. 1992. Neurons immunoreactive to choline acetyltransferase in the turtle retina. Vision Res 32:2023–2030.

Hoskins SG. 1990. Metamorphosis of the amphibian eye. J Neurobiol 21:970–989.

Hutchins JB, Hollyfield JG. 1987. Cholinergic neurons in the human retina. Exp Eye Res 44:363–375.

Lam DM. 1972. Biosynthesis of acetylcholine in turtle photoreceptors. Proc Natl Acad Sci USA 69:1987–1991.

Layer PG. 1991. Cholinesterases during development of the avian nervous system. Cell Mol Neurobiol 11:7–33.

Layer PG, Willbold E. 1994. Cholinesterases in avian neurogenesis. Int Rev Cytol 151:139–181.

Layer PG, Alber R, Rathjen FG. 1988. Sequential activation of butyrylcholinesterase in rostral half somites and acetylcholinesterase in motoneurones and myotomes preceding growth of motor axons. Development 102:387–396.

Layer PG, Weikert T, Alber R. 1993. Cholinesterases regulate neurite growth of chick nerve cells in vitro by means of a non-enzymatic mechanism. Cell Tissue Res 273:219–226.

Layer PG, Berger J, Kinkl N. 1997. Cholinesterases precede "ON-OFF" channel dichotomy in the embryonic chick retina before onset of synaptogenesis. Cell Tissue Res 288:407–416.

Lipton SA, Kater SB. 1989. Neurotransmitter regulation of neuronal outgrowth, plasticity and survival. Trends Neurosci 12:265–270.

Ma PM, Grant P. 1978. Ontogeny of ACh and GABA synthesis during development of the *Xenopus* retina. Brain Res 140:368–373.

Ma PM, Grant P. 1984. Choline acetyltransferase and cholinesterases in the developing *Xenopus* retina. J Neurochem 42:1328–1337.

Mariani AP, Hersh LB. 1988. Synaptic organization of cholinergic amacrine cells in the rhesus monkey retina. J Comp Neurol 267:269–280.

Masland RH. 1977. Maturation of function in the developing rabbit retina. J Comp Neurol 175:275–286.

Masland RH, Livingstone CJ. 1976. Effect of stimulation with light on synthesis and release of acetylcholine by an isolated mammalian retina. J Neurophysiol 39:1210–1219.

Masland RH, Mills JW. 1979. Autoradiographic identification of acetylcholine in the rabbit retina. J Cell Biol 83:159–178.

Masland RH, Mills JW, Hayden SA. 1984. Acetylcholine-synthesizing amacrine cells: identification and selective staining by using radioautography and fluorescent markers. Proc R Soc Lond B Biol Sci 223:79–100.

Massey SC, Redburn DA. 1982. A tonic gamma-aminobutyric acid-mediated inhibition of cholinergic amacrine cells in rabbit retina. J Neurosci 2:1633–1643.

Massey SC, Redburn DA. 1987. Transmitter circuits in the vertebrate retina. Progr Neurobiol 28:55–96.

Meister M, Wong RO, Baylor DA, Shatz CJ. 1991. Synchronous bursts of

action potentials in ganglion cells of the developing mammalian retina. Science 252:939–943.

Millar T, Ishimoto I, Johnson CD, Epstein ML, Chubb IW, Morgan IG. 1985. Cholinergic and acetylcholinesterase-containing neurons of the chicken retina. Neurosci Lett 61:311–316.

Millar TJ, Ishimoto I, Chubb IW, Epstein ML, Johnson CD, Morgan IG. 1987. Cholinergic amacrine cells of the chicken retina: a light and electron microscope immunocytochemical study. Neuroscience 21:725–743.

Negishi K, Wagner HJ. 1995. Differentiation of photoreceptors, glia, and neurons in the retina of the cichlid fish *Aequidens pulcher*: an immunocytochemical study. Brain Res Dev Brain Res 89:87–102.

Nguyen LT, Grzywacz NM. 2000. Colocalization of choline acetyltransferase and γ-aminobutyric acid in the developing and adult turtle retinas. J Comp Neurol 420:527–538.

Penn AA, Riquelme PA, Feller MB, Shatz CJ. 1998. Competition in retinogeniculate patterning driven by spontaneous activity. Science 279: 2108–2112.

Pourcho RG, Osman K. 1986. Cytochemical identification of cholinergic amacrine cells in cat retina. J Comp Neurol 247:497–504.

Redburn DA, Rowe-Rendleman D. 1996. Developmental neurotransmitters. Signals for shaping neuronal circuitry. Invest Ophthalmol Vis Sci 37:1479–1482.

Reese BE, Thompson WF, Peduzzi JD. 1994. Birthdates of neurons in the retinal ganglion cell layer of the ferret. J Comp Neurol 341:464–475.

Reiss Y, Kroger S, Grassi J, Tsim KW, Willbold E, Layer PG. 1996. Extracellular and asymmetric forms of acetylcholinesterase are expressed on cholinergic and noncholinergic terminal neuropil of the developing chick retina. Cell Tissue Res 286:13–22.

Robitzki A, Mack A, Hoppe U, Chatonnet A, Layer PG. 1997. Regulation of cholinesterase gene expression affects neuronal differentiation as revealed by transfection studies on reaggregating embryonic chicken retinal cells. Eur J Neurosci 9:2394–2405.

Sandmann D, Engelmann R, Peichl L. 1997. Starburst cholinergic amacrine cells in the tree shrew retina. J Comp Neurol 389:161–176.

Schmidt M, Wassle H, Humphrey M. 1985. Number and distribution of putative cholinergic neurons in the cat retina. Neurosci Lett 59:235–240.

Schwartz IR, Bok D. 1979. Electron microscopic localization of [125I]alpha-bungarotoxin binding sites in the outer plexiform layer of the goldfish retina. J Neurocytol 8:53–66.

Sernagor E, Grzywacz NM. 1995. Emergence of complex receptive field properties of ganglion cells in the developing turtle retina. J Neurophysiol 73:1355–1364.

Sernagor E, Grzywacz NM. 1996. Influence of spontaneous activity and visual experience on developing retinal receptive fields. Curr Biol 6:1503–1508.

Sernagor E, Grzywacz NM. 1999. Spontaneous activity in developing turtle retinal ganglion cells: pharmacological studies. J Neurosci 19:3874–3887.

Small DH, Michaelson S, Sberna G. 1996. Non-classical actions of cholinesterases: role in cellular differentiation, tumorigenesis and Alzheimer's disease. Neurochem Int 28:453–483.

Smith J, Fauquet M, Ziller C, Le Douarin NM. 1979. Acetylcholine synthesis by mesencephalic neural crest cells in the process of migration in vivo. Nature 282:853–855.

Spira AW, Millar TJ, Ishimoto I, Epstein ML, Johnson CD, Dahl JL, Morgan IG. 1987. Localization of choline acetyltransferase-like immunoreactivity in the embryonic chick retina. J Comp Neurol 260:526–538.

Sprent P. 1993. Applied nonparametric statistical methods. London: Chapman and Hall.

Tauchi M, Masland RH. 1984. The shape and arrangement of the cholinergic neurons in the rabbit retina. Proc R Soc Lond B Biol Sci 223:101–119.

Vaney DI. 1984. "Coronate" amacrine cells in the rabbit retina have the "starburst" dendritic morphology. Proc R Soc Lond B Biol Sci 220:501–508.

Vaney DI. 1990. The mosaic of amacrine cells in the mammalian retina. In: Osborne N, Chader J, editors. Progress in retinal research. Oxford: Pergamon Press. p 49–100.

Vaney DI, Peichl L, Boycott BB. 1981. Matching populations of amacrine cells in the inner nuclear and ganglion cell layers of the rabbit retina. J Comp Neurol 199:373–391.

Voigt T. 1986. Cholinergic amacrine cells in the rat retina. J Comp Neurol 248:19–35.

Wong RO. 1995. Cholinergic regulation of [Ca2+]i during cell division and differentiation in the mammalian retina. J Neurosci 15:2696–2706.

Wong RO, Meister M, Shatz CJ. 1993. Transient period of correlated bursting activity during development of the mammalian retina. Neuron 11:923–938.

Wong RO, Chernjavsky A, Smith SJ, Shatz CJ. 1995. Early functional neural networks in the developing retina. Nature 374:716–718.

Yntema CL. 1968. A series of stages in the embryonic development of *Chelydra serpentina*. J Morphol 125:219–251.

Zhou ZJ. 1998. Direct participation of starburst amacrine cells in spontaneous rhythmic activities in the developing mammalian retina. J Neurosci 18:4155–4165.